Anelastic Model of a Twin Accumulator Hydro-pneumatic Suspension System

C.L. Giliomee[1], P.S. Els[2] and J.L. van Niekerk[3]

This paper describes the mathematical model of an anelastic model for a twin accumulator hydro-pneumatic suspension system, verified with experimental data. A methodology for determining the (linear) characteristics for the series spring/damper is also supplied and the results are compared to measurements done on a laboratory set-up. Good correlation is obtained between measured data and the analysis results for triangular displacement inputs at different excitation frequencies. The twin accumulator model is very basic and can be expanded to model a semi-active hydro-pneumatic suspension, by the addition of extra force elements.

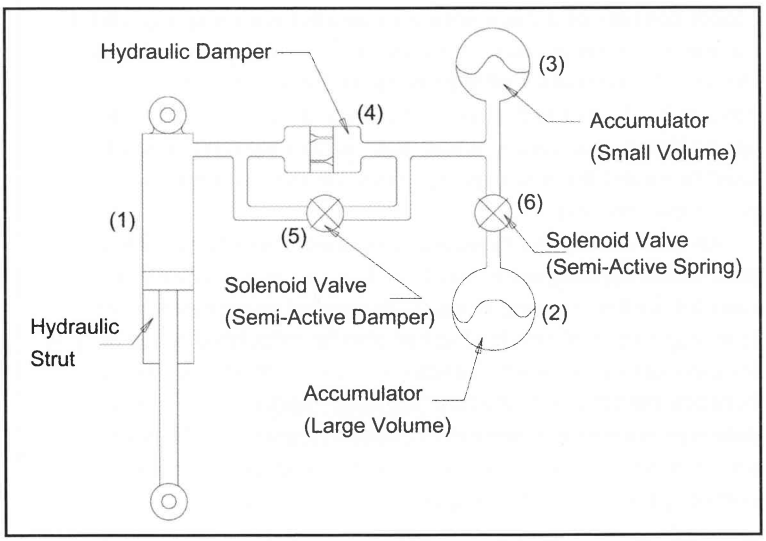


Figure 1: Schematic layout of the semi-active spring/damper system

NOMENCLATURE

A Accumulator floating piston area $[m^2]$
F Force $[N]$
P Pressure $[Pa]$
b Polytropic constant (function of static volume and pressure)
c Damping constant $[Ns/m]$
k Spring stiffness $[N/m]$
n Polytropic exponent
x Displacement $[m]$

1 Introduction

Passive suspension systems (suspensions with no controllable elements) always lead to a compromise between ride comfort and handling, since a stiff suspension is required for good handling, while a more compliant suspension improves ride comfort. Implementing a controllable suspension is therefore an attempt to deal with these opposing requirements for improved ride comfort and handling by providing the opportunity to adjust the suspension settings dependent on the current road and driver inputs to the vehicle.

The semi-active suspension system is shown in Figure 1 and works as follows: The switching between high and low characteristics for both the spring and the damper characteristics is made possible by redirecting the hydraulic fluid with two solenoid valves. The spring/damper unit consists of a hydraulic strut[1], two Nitrogen filled accumulators[2,3], a hydraulic damper[4] and the two solenoid valves[5,6]. The low spring rate is achieved by compressing a large volume of gas, consisting of two separate accumulators[2,3]. By closing off one of the accumulators[2], a smaller gas volume[3] is compressed and hence a higher spring rate is achieved. Spring rates can be individually tailored by changing the two gas volumes when the system is designed. For low damping the hydraulic damper[4] is short-circuited by opening a by-pass valve[5]. For high damping this valve is closed and the hydraulic fluid is forced through the damper resulting in a higher damping force.

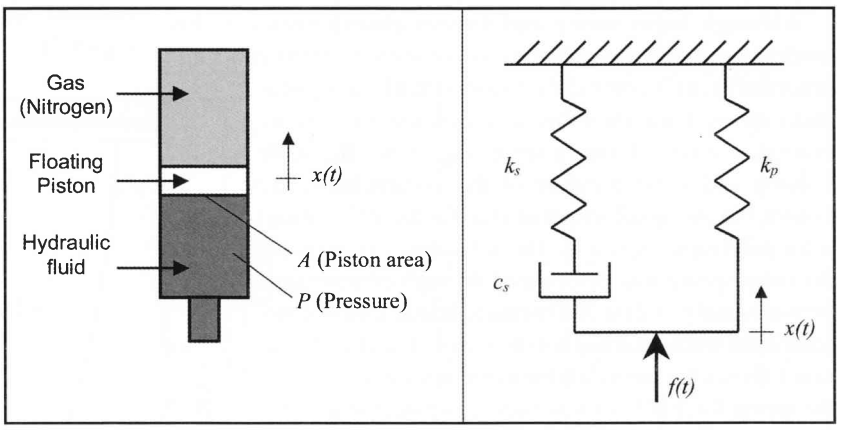


Figure 2: Basic anelastic spring model

This paper will however focus on the system without any control valves and will therefore model the semi-active system in the off state, i.e. all valves open. In addition, the hydraulic damper is also omitted in order to focus on the twin accumulators.

The anelastic approach to model a twin accumulator system was chosen since a hyteresis loop, as typically found in hydro-pneumatic springs, can easily be replicated by an anelastic

[1] Department of Mechanical and Aeronautical Engineering, University of Pretoria, Pretoria, 0002, South Africa, Tel: +27-12-345-5129, Fax: +27-12-345-5034, E-mail: chris@lmt.co.za
[2] Department of Mechanical and Aeronautical Engineering, University of Pretoria, Pretoria, 0002, South Africa, Tel: +27-12-420-2045, Fax: +27-12-362-5087, E-mail: schalk.els@eng.up.ac.za
[3] Department of Mechanical Engineering, Stellenbosch University, Private Bag X1, Matieland 7602, South Africa, Tel: +27-21-808-4251, Fax: +27-21-808-4958, E-mail: wikus@sun.ac.za

spring model. Obtaining the desired characteristics for the spring and damper coefficients are however more difficult, and will be discussed in more detail in the remainder of this article. The twin accumulator anelastic model consists of two anelastic spring models, one for each of the accumulators. Each anelastic model consists of a main spring in parallel with a spring and damper set in series. Before the anelastic model can be solved the six characteristics of the spring and damper components have to be determined. Linear characteristics are used for the spring/damper in series, while non-linear characteristics are used to model the main spring, based on the assumption of a polytropic process.

An overview of the basic anelastic model will be provided, after which the main spring model will be discussed. The parameters for the linear spring/damper characteristics are determined from experimental results, but can also be calculated based on the thermal time constant, as explained by Els (1993). Correlation between the twin accumulator anelastic model and measured data is provided for a range of excitation frequencies. Only one set of model parameters was used to produce the analysis outputs presented in this paper.

2 Mathematical models

2.1 Basic anelastic model

The anelastic model is well known and is used, amongst others, to model viscoelasticity, creep, material relaxation, thermal processes and other time dependent processes. An example of where the anelastic model was used to model a gas spring can be found in Kronhauser 1994.

Figure 2 shows schematic representations of the anelastic model for a single hydro-pneumatic spring, as first proposed by Pourmovahed and Otis (1984). From this figure, it can be seen that the anelastic model consists of a spring in parallel with a spring and damper, which are in series. Through inspection it is possible to see that the basic spring stiffness is supplied by spring k_p (main spring), while the hysteresis loop will be produced by the series spring and damper combination (k_s and c_s).

Although linear spring and damper characteristics in this model also produce a hysteresis loop, the characteristics are not progressive, as is commonly found with a hydro-pneumatic spring. It was therefore decided to use a polytropic process to model the main spring (k_p). Since the static volume and static pressure of the accumulators are known, the one unknown parameter (for the main spring) is the polytropic exponent. The polytropic exponent for the main spring was determined through comparisons between analysis data and measured data. Linear characteristics were assumed for the series elements. Equation 1 shows the formula which can be used to calculate the spring force (F) as a function of displacement (x) for the main spring (k_p). This formula is obtained from the equation for the polytropic process, i.e. $PV^n=b$, where b is constant. In equation 1, b is the constant calculated from the initial pressure (P), volume (V) and polytropic exponent (n).

$$f(t)=\frac{bA}{(xA)^n} \qquad (1)$$

The anelastic model however requires a spring constant for the main spring; therefore equation 1 was differentiated once with respect to displacement to obtain a function for the main spring stiffness. The non-linear spring stiffness is given by the function:

$$\frac{df(x)}{dx}=-nbA^{(1-n)}(x-x_0)^{(-n-1)} \qquad (2)$$

where x_0 is the static displacement and x is the dynamic displacement. The reason for introducing the static displacement is to model the static volume of the accumulator, i.e. when x is zero, Ax_0 represents the static accumulator volume.

As can be seen from the above equation, the main spring stiffness is a function of the polytropic exponent, the polytropic constant, the piston area and piston displacement (refer to Figure 2).

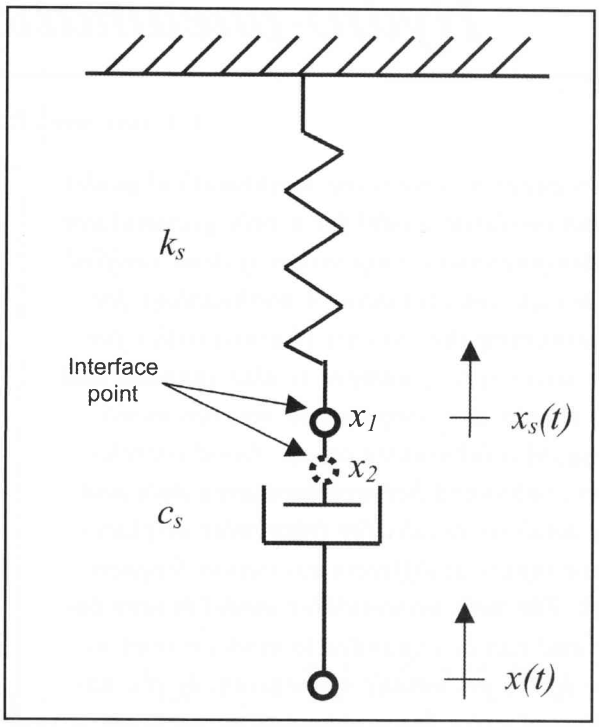


Figure 3: Series spring/damper model

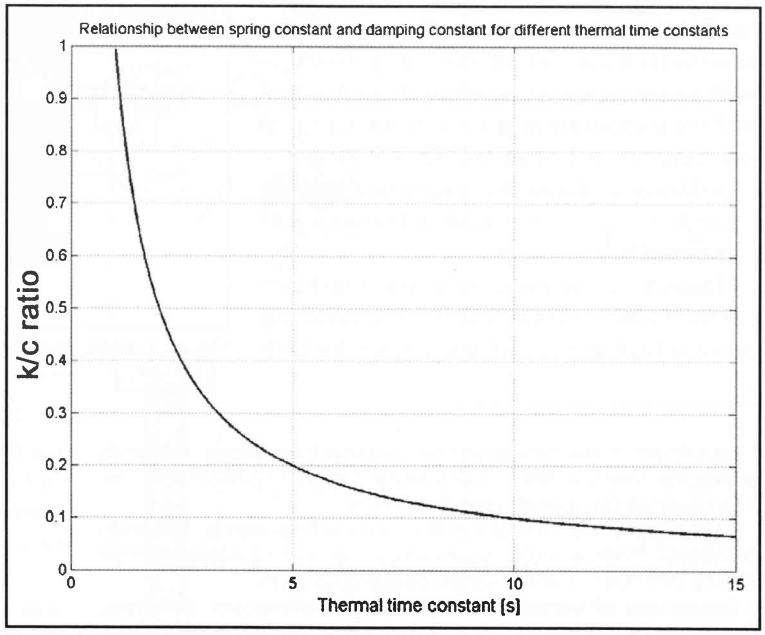
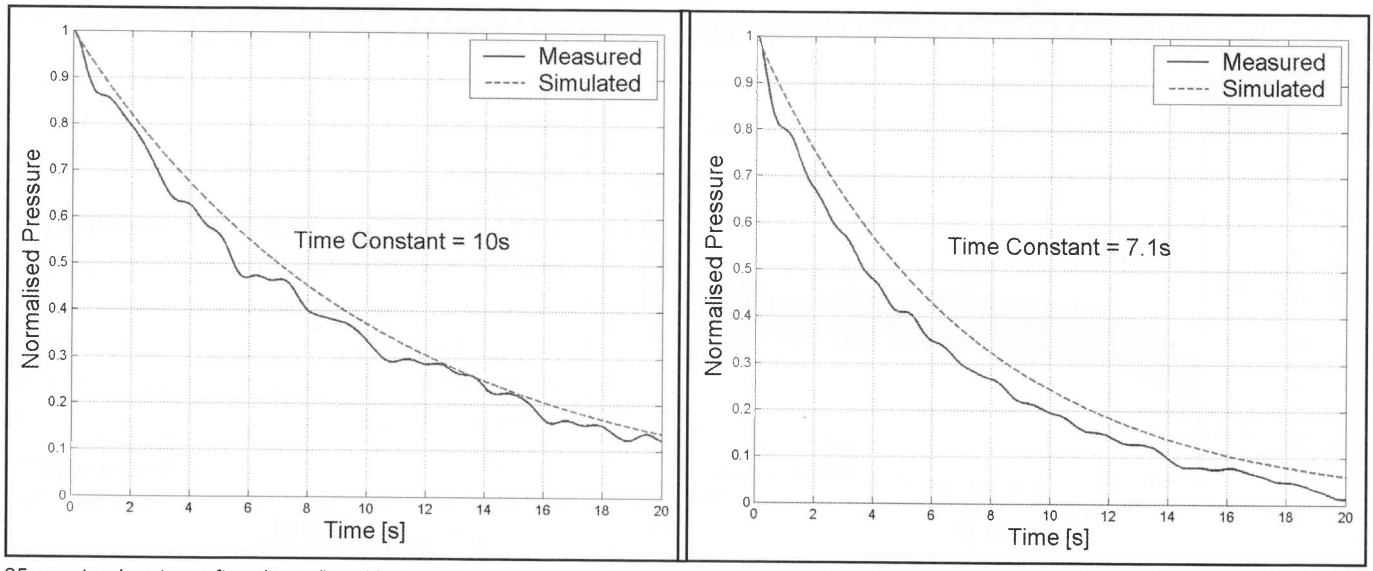


Figure 4: Graph of *k/c* ratio



25mm step input – soft spring, c/k = 10.1

50mm step input – soft spring, c/k = 7.1

Figure 5: Decay correlation between measured and simulated response to a step input

2.2 Series spring/damper parameters

As mentioned previously, linear characteristics were assumed for the series spring/damper combination. The relationship between the spring stiffness and damper coefficient can be determined by viewing the series spring/damper system in isolation. The aim is to get the spring/damper system to mimic the relaxation behaviour of a hydro-pneumatic spring for a step input. Figure 3 shows a schematic layout of the series spring/damper.

Assume that the system starts in a state just after a step input at x(t). From a force balance at the interface point between the spring and the damper, the following equation can be deduced (assume that the mass at the interface point is negligible).

$$k_s x(t) = c_s\left[\dot{x}(t) - \dot{x}_s(t)\right]$$

For a unit step input in the displacement $x(t)$ (with $x(t)$after the initial input) it is easy to show that the solution is given by:

$$x_s(t) = \exp\left(-\frac{k_s}{c_s}t\right)$$

or,

$$x_s(t) = \exp\left(-\frac{t}{\tau}\right)$$

where $\tau = \frac{c_s}{k_s}$ is the time constant of the first order system, which is similar to the definition of the thermal time constant, Els 1993. Rewriting it as a ratio of stiffness to damping:

$$\frac{k_s}{c_s} = \frac{1}{\tau} \qquad (3)$$

Figure 4 shows a graphical representation of equation 3. From this figure, it can be seen that for a thermal time constant of say 6*s*, the k_s/c_s ratio is 0.166; therefore the damping constant must be six times larger than the spring constant to obtain the same decay behaviour that a 6*s* thermal time constant would produce. The thermal time constant can be determined experimentally, or through calculations (Pourmovahed and Otis, 1990).

The series spring/damper behaviour was verified with measured data. Since force and pressure is a scalar product of the displacement of the spring/damper interface point, analysis results were compared with measurements, by reducing both the test data and the analysis data to a normalised pressure. Figure 5 shows two cases, one for a 25mm and one for a 50mm step input. Since the normalised pressures are compared in Figure 5, arbitrary values were chosen for k and c, while the c/k ratio corresponding to the relevant time constant was used (refer to Figure 5).

2.3 Twin accumulator anelastic model

For the twin accumulator model, the two anelastic systems (one

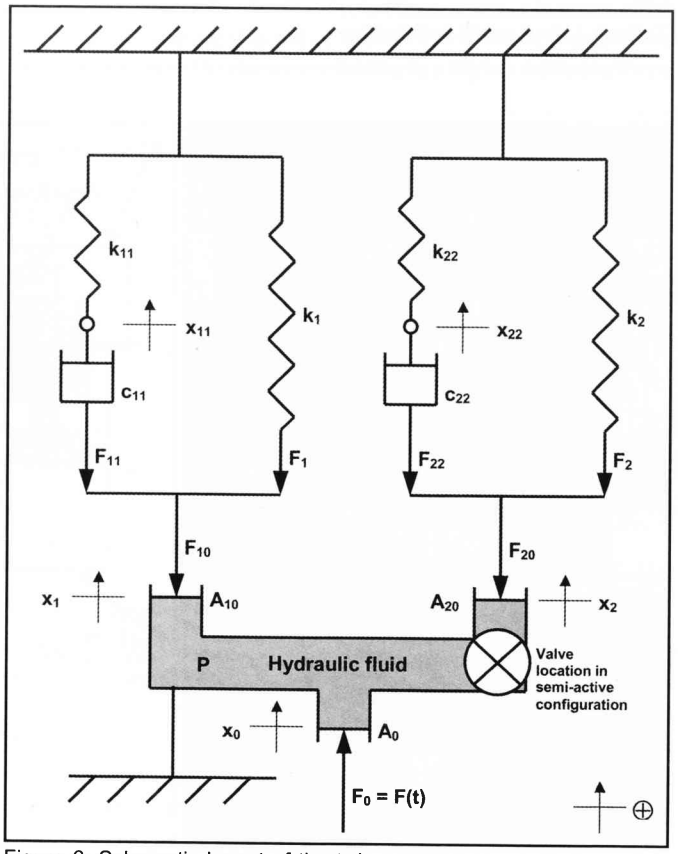


Figure 6: Schematic layout of the twin accumulator anelastic model

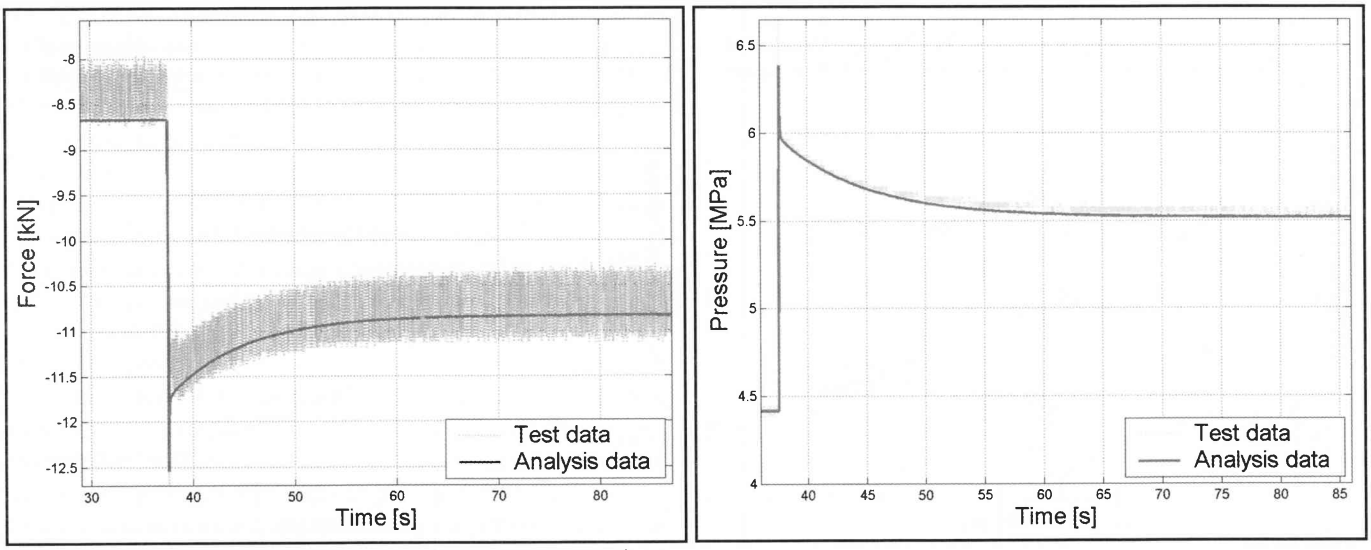


Figure 7: Correlation graphs for a step input (time constant test)

Parameter	Value	Units
n (both accumulators)	1.85	-
b (small volume - 0.1 litre)	0.1811	(calculated with SI units)
b (large volume - 0.4 litre)	2.354	(calculated with SI units)
P (static)	4.55	*MPa*
k_{11}	3.5e5	*N/m*
k_{22}	3.5e5	*N/m*
c_{11}	2.49e6 (7.1xk_{11})	*Ns/m*
c_{22}	2.49e6 (7.1xk_{11})	*Ns/m*

Table 1: List of model parameters

for each accumulator) are combined in a single model, which incorporates a hydraulic T branch to split the force equally between the two accumulators. Figure 6 shows a schematic layout of the twin accumulator anelastic model, that was used to derive the equations for solving this model. The derivation of the mathematical model is supplied in Appendix A. From Appendix A, it can be seen that ten algebraic and two differential equations describe the force and displacement characteristics of the twin accumulator anelastic model. The algebraic equations are solved through matrix manipulation, while the ODE45 function in Matlab is used to solve the differential equations.

A list of the parameters used for the twin accumulator anelastic model is supplied in Table 1.

The values for k_{11} and k_{22} were determined by comparing analysis data with measured data for a displacement step input. The values supplied in Table 1 gives the same force and pressure decay as was measured on the experimental setup. Figure 7 shows the correlation between measured and simulation data for a step displacement input of approximately 50mm. The step input experiment is used to determine the thermal time constant of a system, as explained by Els (1993).

3 Test setup

The analysis results presented in this document are correlated with measurements taken on a prototype semi-active hydropneumatic system. Figure 8 show a photograph of the test configuration, as well as a schematical layout. In order to compare measurements with analysis data, the semi-active

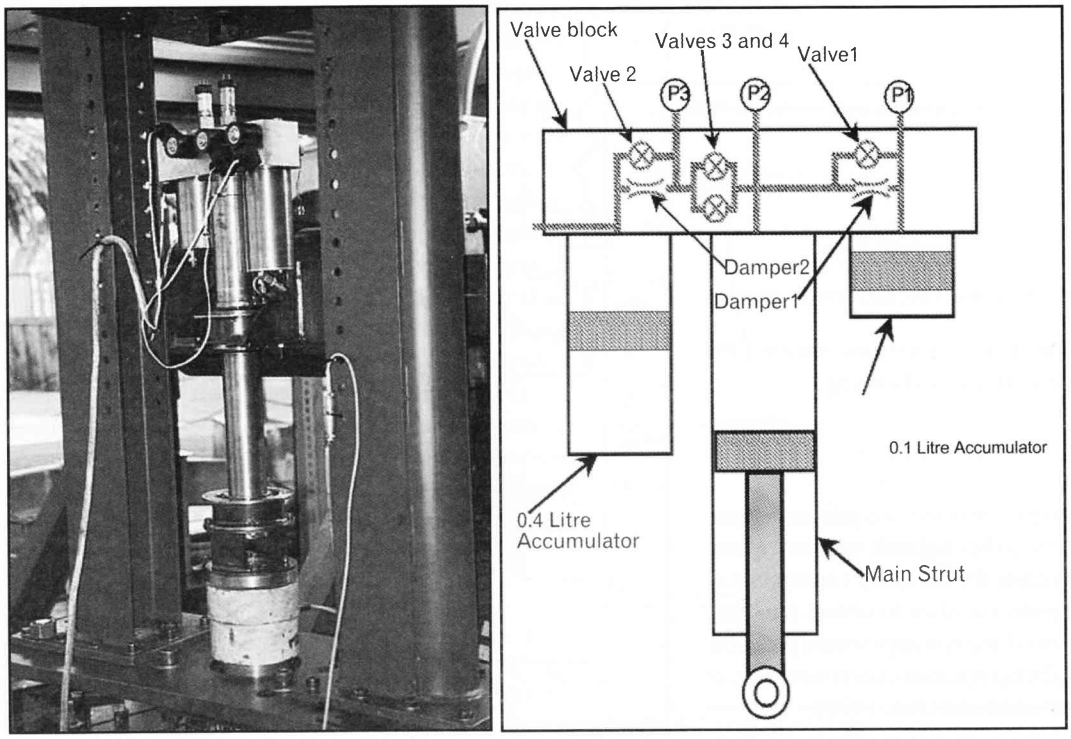


Figure 8: Test configuration

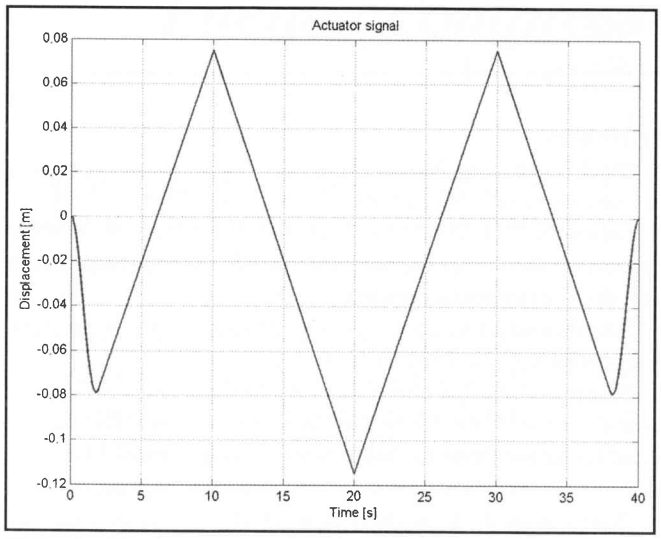


Figure 9: Actuator signal

hydro-pneumatic spring was tested in the passive state, i.e. all the valves (Valve 1 to Valve 4) were kept open during the tests. The tests were performed on a $160kN$ Schenck hydraulic actuator. Pressures, as indicated in Figure 8, as well as actuator force, actuator displacement, valve switching signal and Valve 3 displacement were measured.

4 Correlation

Five tests were performed with a triangular displacement input (with sinusoidal ramps at either end) at different excitation frequencies. The reason for using a triangular displacement input is to keep the input velocity constant. Figure 9 shows a typical actuator displacement input signal used during the tests. The same signal was used as input for the simulation model.

Correlation figures of strut force and pressure are supplied in Appendix B for excitation frequencies of $0.001Hz, 0.01Hz, 0.05Hz, 0.1Hz$ and $0.5Hz$. From these figures, it can be seen that there is good correlation between the measured data and the analysis results. The simulation model however fails to predict the sudden change in force/pressure at the turning points. A possible reason for this is that the mathematical model does not take into account friction, since this phenomenon can be seen more clearly on the force graphs than the pressure graphs.

5 Conclusions

In this paper, the twin accumulator anelastic model was discussed and measured data was compared with analysis results. The mathematical model was verified with measured data. The model can be expanded to take into account phenomena such as friction and the bulk modulus of the oil by the addition of extra force elements in the mathematical model.

Currently the polytropic exponent and the series spring (or damper) constants are determined through curve fitting test data to the analysis data. The relationship between the two variables, polytropic exponent and series spring constants, and the mechanical (or thermal) time constant should be investigated in more detail. A variable time constant can also be implemented, which could improve on the correlation obtained in this study.

The mathematical model is computationally efficient and solves faster than real time on an Intel P4 PC with 512Mb RAM.

Appendix A: Twin accumulator anelastic mathematical model derivation.

With reference to Figure 6, the following equations can be written:

Algebraic equations

$$F_{11} = -k_{11}x_{11} = c_{11}(\dot{x}_1 - \dot{x}_{11}) \quad (1)$$

$$F_{22} = -k_{22}x_{22} = c_{22}(\dot{x}_2 - \dot{x}_{22}) \quad (2)$$

$$F_1 = -k_1x_1 \quad (3)$$

$$F_2 = -k_2x_2 \quad (4)$$

$$F_{10} = F_{11} + F_1 \quad (5)$$

$$F_{20} = F_{22} + F_2 \quad (6)$$

$$F_{10} = PA_{10} \quad (7)$$

$$F_{20} = PA_{20} \quad (8)$$

$$F_0 = PA_0 \quad (9)$$

$$x_0 = A_{10}/A_0 x_1 + A_{20}/A_0 x_2 \quad (10)$$

With:

Variables:

$F_0, F_1, F_2, F_{11}, F_{22}, F_{10}, F_{20}, x_1, x_2, P$

Inputs:

x_0

In matrix format these equations are:

$$\begin{bmatrix} 0 & 0 & 0 & 1 & 0 & 0 & 0 & 0 & 0 & 0 \\ 0 & 0 & 0 & 0 & 1 & 0 & 0 & 0 & 0 & 0 \\ 0 & 1 & 0 & 0 & 0 & 0 & 0 & -k_1 & 0 & 0 \\ 0 & 0 & 1 & 0 & 0 & 0 & 0 & 0 & -k_2 & 0 \\ 0 & -1 & 0 & -1 & 0 & 1 & 0 & 0 & 0 & 0 \\ 0 & 0 & -1 & 0 & -1 & 0 & 1 & 0 & 0 & 0 \\ 0 & 0 & 0 & 0 & 0 & 1 & 0 & 0 & 0 & -A_{10} \\ 0 & 0 & 0 & 0 & 0 & 0 & 1 & 0 & 0 & -A_{20} \\ 1 & 0 & 0 & 0 & 0 & 0 & 0 & 0 & 0 & -A_0 \\ 0 & 0 & 0 & 0 & 0 & 0 & 0 & A_{10}/A_0 & A_{20}/A_0 & 0 \end{bmatrix} \begin{Bmatrix} F_0 \\ F_1 \\ F_2 \\ F_{11} \\ F_{22} \\ F_{10} \\ F_{20} \\ x_1 \\ x_2 \\ P \end{Bmatrix} = \begin{bmatrix} k_{11}x_{11} \\ k_{22}x_{22} \\ 0 \\ 0 \\ 0 \\ 0 \\ 0 \\ 0 \\ 0 \\ x_0 \end{bmatrix}$$

Since a polytropic process was used for the main springs (k_1 and k_2), and the above equations only require spring stiffness, the polytropic equation was differentiated to obtain the polytropic stiffness function. The following equation was therefore used to determine the main spring stiffness as a function of polytropic exponent (n), polytropic constant (b), piston area (A), static or initial displacement (x_0) and the floating piston displacement (x).

$$f'(x) = -nbA^{(1-n)}(x - x_0)^{(-n-1)}$$

Differential equations:

$$\dot{x}_{11} = -\frac{k_{11}}{c_{11}} x_{11} + \dot{x}_1 \quad (10)$$

$$\dot{x}_{22} = -\frac{k_{22}}{c_{22}} x_{22} + \dot{x}_2 \quad (11)$$

In state-space format these equations are:

$$\dot{X} = \begin{bmatrix} -\frac{k_{11}}{c_{11}} & 0 \\ 0 & -\frac{k_{22}}{c_{22}} \end{bmatrix} X + \begin{bmatrix} \dot{x}_1 \\ \dot{x}_2 \end{bmatrix}$$

With

$$X = [x_{11} \quad x_{22}]^T$$

References

1. Els, P S 1993. *Die Hitteprobleem op Hidropneumatiese Veer-en-Demperstelsels.* MEng thesis. University of Pretoria, Pretoria.
2. Giliomee, C L 2003. *Analysis of a Four State Switchable Hydro-pneumatic Spring and Damper System.* MEng thesis. University of Pretoria, Pretoria.
3. Kronhauser, AA 1994. *Dynamic Modeling of Gas Springs.* Transactions of the ASME 116, 414-418.
4. Pourmovahed, A & Otis, D R 1990. *An Experimental Thermal Time-Constant Correlation for Hydraulic Accumulators.* Journal of Dynamic Systems, Measurement, and Control 112, 116-121.
5. Pourmovahed, A & Otis, D R 1984. *Effects of Thermal Damping on the Dynamic Response of a Hydraulic Motor-Accumulator System.* Journal of Dynamic Systems, Measurement, and Control 106, 21-26.

Appendix B: Correlation of experimental and analysis results

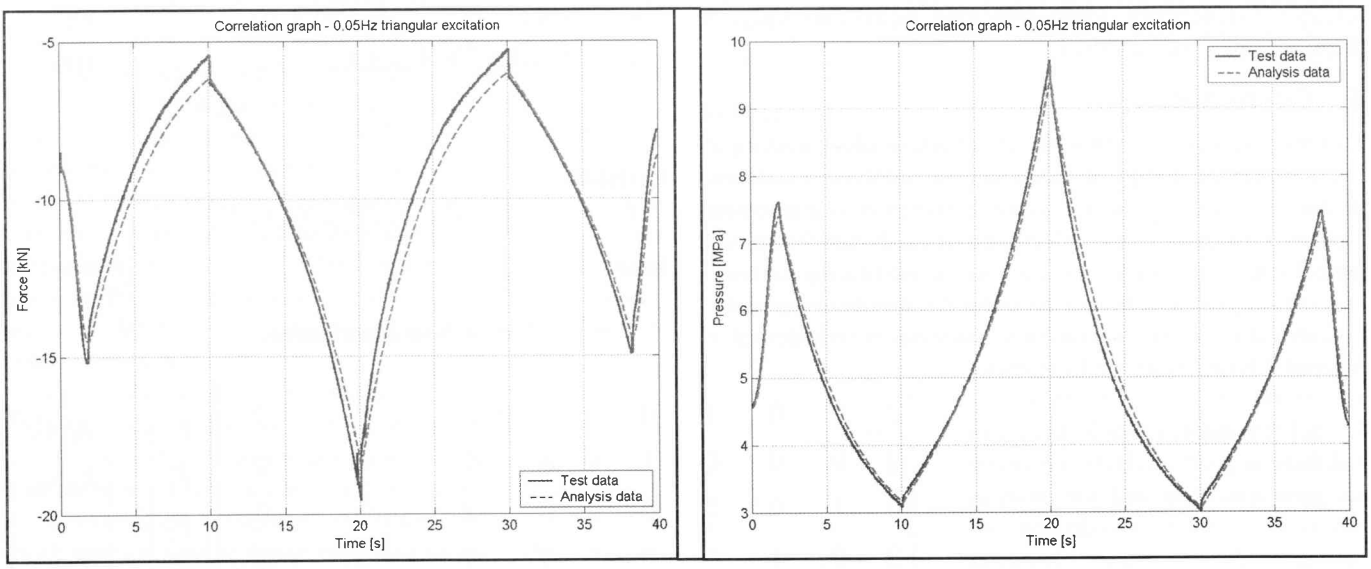


Figure 10: 0.001Hz excitation

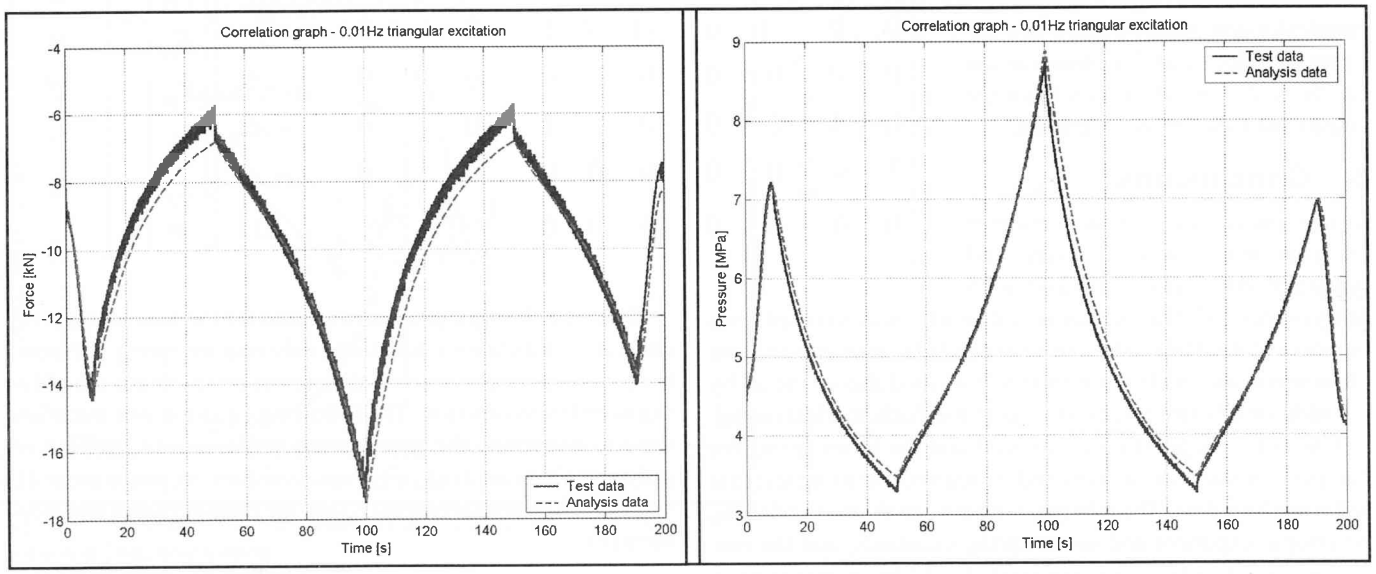


Figure 11: 0.01Hz excitation

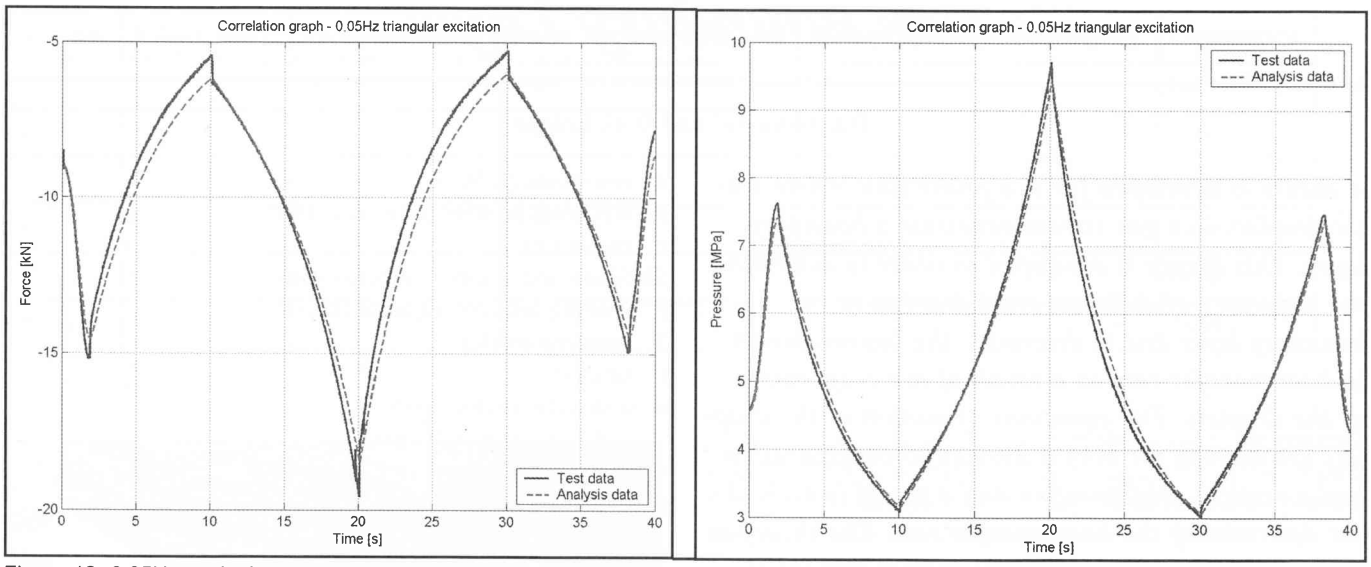


Figure 12: 0.05Hz excitation

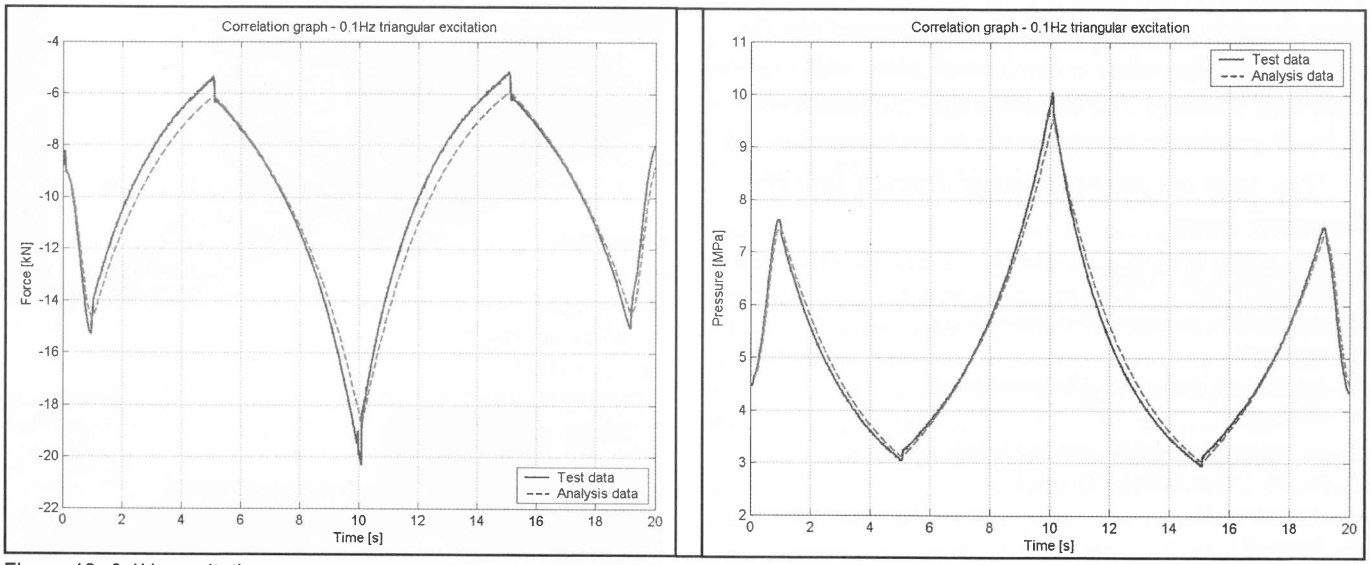


Figure 13: 0.1Hz excitation

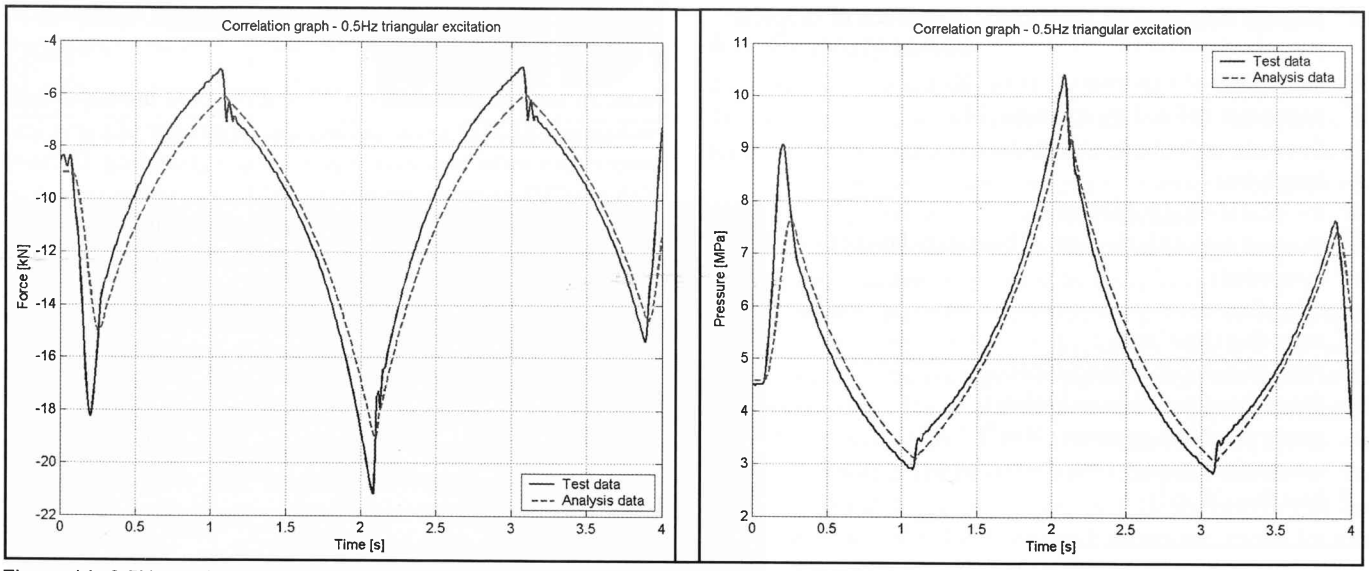


Figure 14: 0.5Hz excitation